

Electron kinetics in low-temperature plasmas

Cite as: Phys. Plasmas **26**, 060601 (2019); <https://doi.org/10.1063/1.5093199>

Submitted: 18 February 2019 • Accepted: 05 May 2019 • Published Online: 04 June 2019

 Vladimir Kolobov and  Valery Godyak



View Online



Export Citation



CrossMark

ARTICLES YOU MAY BE INTERESTED IN

[Electron dynamics in low pressure capacitively coupled radio frequency discharges](#)
Journal of Applied Physics **127**, 181101 (2020); <https://doi.org/10.1063/5.0003114>

[On the generalized formulation of Debye shielding in plasmas](#)
Physics of Plasmas **26**, 050701 (2019); <https://doi.org/10.1063/1.5091949>

[Perspectives, frontiers, and new horizons for plasma-based space electric propulsion](#)
Physics of Plasmas **27**, 020601 (2020); <https://doi.org/10.1063/1.5109141>



Physics of Plasmas
Features in Plasma Physics Webinars

Register Today!



Electron kinetics in low-temperature plasmas

Cite as: Phys. Plasmas **26**, 060601 (2019); doi: [10.1063/1.5093199](https://doi.org/10.1063/1.5093199)

Submitted: 18 February 2019 · Accepted: 5 May 2019 ·

Published Online: 4 June 2019



View Online



Export Citation



CrossMark

Vladimir Kolobov^{1,2,a)}  and Valery Godyak^{3,4,b)} 

AFFILIATIONS

¹CFD Research Corporation, Huntsville, Alabama 35806, USA

²The Center for Space Plasma and Aeronomic Research, The University of Alabama in Huntsville, Huntsville, Alabama 35899, USA

³The Electrical Engineering and Computer Science Department, University of Michigan, Ann Arbor, Michigan 48109, USA

⁴RF Plasma Consulting, Brookline, Massachusetts 02446, USA

^{a)}vladimir.kolobov@cfdr.com

^{b)}egodyak@comcast.net

ABSTRACT

This article presents an overview of recent advances in the field of electron kinetics in low-temperature plasmas (LTPs). It also provides author's views on where the field is headed and suggests promising strategies for further development. The authors have selected several problems to illustrate multidisciplinary nature of the subject (space and laboratory plasma, collisionless and collisional plasmas, and low-pressure and high-pressure discharges) and to illustrate how cross-disciplinary research efforts could enable further progress. Nonlocal electron kinetics and nonlocal electrodynamics in low-pressure rf plasmas resemble collisionless effects in space plasma and hot plasma effects in fusion science, terahertz technology, and plasmonics. The formation of electron groups in dc and rf discharges has much in common with three groups of electrons (core, strahl, and halo) in solar wind. Runaway electrons in LTPs are responsible for a wide range of physical phenomena from nano- and picoscale breakdown of dielectrics to lightning initiation. Understanding electron kinetics of LTPs could promote scientific advances in a number of topics in plasma physics and accelerate modern plasma technologies.

Published under license by AIP Publishing. <https://doi.org/10.1063/1.5093199>

I. INTRODUCTION

Low-Temperature Plasmas (LTPs) can be broadly defined as plasmas with electron energies of the order of ionization potential of atoms and molecules (about 10 eV). Indeed, a small number of super-thermal electrons could have energies up to several kilo-electron-volts, typical of runaway electrons (RE) in gas discharges and solar wind electrons. Most fundamental properties of LTPs are due to the distinction of electron mass and the masses of ions and neutrals. LTPs could be weakly ionized and collisional, as in gas discharges, or fully ionized and collisionless, as in space. However, collisionless space plasmas often demonstrate collisional behavior due to wave-particle interactions and turbulence, whereas collisional discharge plasmas exhibit collisionless phenomena such as stochastic electron heating and an anomalous skin effect.

The common feature of all LTPs is their nonequilibrium nature.¹ In particular, electrons are far from equilibrium with ions and neutrals. They are even not in equilibrium within their own ensemble, and they can be out of equilibrium with electric fields that maintain the plasma. The main causes of electron nonequilibrium are: (a) large spatial gradients, (b) strong electric fields, (c) fast temporal variations, and (d)

collisions with neutral plasma species. The last point indicates that, even for a spatially uniform, steady plasma, the dominance of electron collisions with neutrals and, specially, inelastic collisions, over Coulomb interactions guarantees a non-Maxwellian electron distribution function (EDF) in weakly ionized plasma. The non-Maxwellian distributions are also well known for space plasmas. In particular, the formation of three groups of electrons (core, strahl, and halo) in solar wind has deep similarities with the formation of three electron groups in gas discharges. Therefore, the electron distribution function (EDF) is non-Maxwellian in general.

However, many of the plasma parameter definitions are based on the assumption of a Maxwellian EDF. As discussed above, this assumption is not valid under most of the relevant gas discharge and space plasma conditions. For a non-Maxwellian EDF, the electron temperature T_e is losing its usual meaning and implies a mean electron energy $T_{\text{eff}} = 2/3 \langle \epsilon \rangle$. Many plasma parameters and rates of electron-induced chemical reactions calculated with T_e found from a narrow portion of the real EDF (with standard probes or spectroscopy) may be in strong disagreement with those calculated with the realistic EDF. It is known that T_{eff} plasma conductivity σ_p , Debye length λ_D , and the ion sound speed v_s are mainly defined by the low-energy part of the

EDF, while inelastic collision rates and floating wall potential (responsible for the electron flux to the wall) are most sensitive to the EDF shape at high electron energies. In order to accurately determine these plasma parameters and the rates of electron induced processes, the EDF should be calculated and diagnosed using adequate kinetic models and experimental techniques.

A kinetic description of LTP implies solving the Boltzmann equation for the velocity distribution functions of electrons, ions, and neutral species. There has been impressive progress in the kinetic theory^{2,3} and simulations of gas discharges using particle-based methods^{4,5} and mesh-based kinetic solvers.^{6,7} Under certain circumstances, simpler hydrodynamic (fluid) descriptions can be applied.⁸ Deep understanding of the particle kinetics is required for identifying the applicability of the fluid description and selecting appropriate closure models. The latter depend on plasma conditions (collisionless vs collisional, magnetized vs nonmagnetized), the particle type, and energy. Development of hybrid kinetic-fluid plasma models is a subject of active research.⁹

The classical experimental techniques like Langmuir probes and spectroscopy (both based on the assumption of a Maxwellian EDF) being the main instruments for plasma parameter diagnostics during the last century appeared to be inadequate for diagnostics of plasmas with a non-Maxwellian EDF. Detailed studies by different authors revealed significant errors in probe diagnostics, based on electron and ion parts of the probe characteristic, for non-Maxwellian plasmas.

Among three known ways of EDF diagnostics; Langmuir-Druyvesteyn, plasma spectroscopy, and Thompson scattering, only the first one is well developed and suitable for reliable measurement of the isotropic EDF in a wide range of discharge conditions and electron energies. Plasma spectroscopy misses the low-energy part of the EDF where the majority of electrons reside and it only provides spatially averaged information on the EDF rather than a localized one. Thomson scattering tends to miss the high-energy part of the EDF responsible for excitation, ionization, and electron-induced chemical

reactions due to its lower signal to noise ratio in the high energy part of the spectra. In contrast, the probe measurements of the EDFs^{10,11} revealed the heating mode transitions with an abundance of cold electrons in rf capacitive (CCP), and inductive plasma (ICP), the paradoxical T_e distribution in CCP,¹² and the absence of the Maxwellian EDF under conditions of Langmuir paradox.¹³ Examples of typical non-Maxwellian EDFs in argon CCP and ICP are given in Fig. 1.

Over the last three decades, substantial progress has been achieved in understanding electron kinetics and electrodynamics of gas discharges.^{10,11,14–19} It was recognized that electron thermal motion plays a fundamental role in plasma electrodynamics at low gas pressures. At the end of the 20th century, collisionless electron heating and negative power absorption under conditions of an anomalous skin effect and a nonlinear skin effect associated with rf magnetic field were recognized as an essential part of ICP physics at low gas pressures. It was found that the rf magnetic field, which is responsible for the ICP maintenance, can be completely absent in rf plasma, or play a crucial role in electron kinetics in the skin layer, through nonlinear effects such as second harmonic currents and ponderomotive forces, or through magnetization of electrons during some parts of the rf period and demagnetization during other parts (at low driving frequencies). “However, most of these effects are still ignored in the computer codes for gas discharge plasmas used in semiconductor technology and in positive and negative ion sources for particle acceleration and space propulsion.”

Another example of the electron kinetic effect is plasma stratification.²⁰ Striations have been observed in dc and rf discharges of atomic and molecular gases since the 19th century. Although most types of striations (ionization waves) in noble gases have been understood by the end of the 20th century, only one type of moving striation has been successfully reproduced in computer simulations. Striations in rf discharges and in molecular gases that frequently occurred in industrial and laboratory plasmas are not understood, even at a qualitative level. Plasma stratification, as an example of self-organization at the

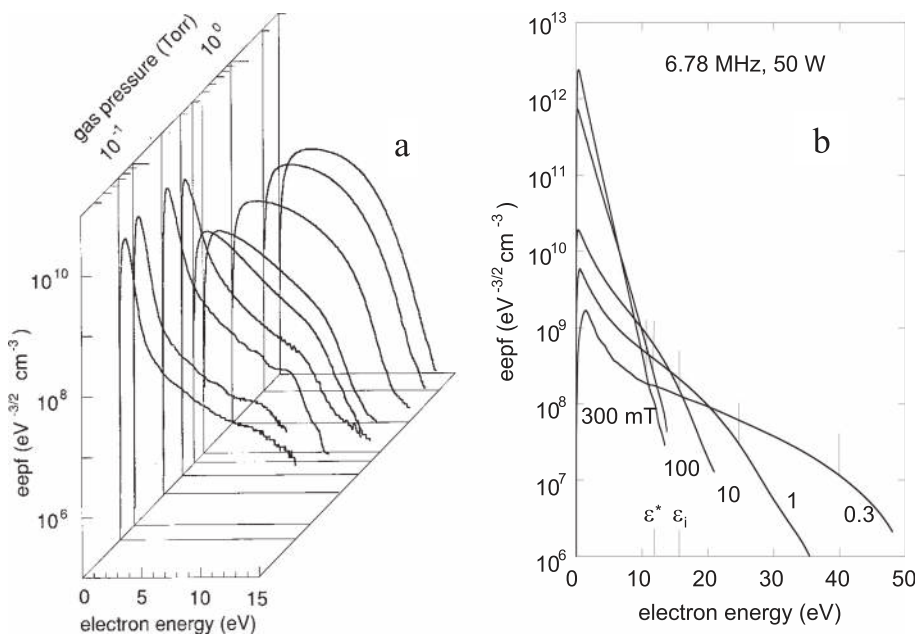


FIG. 1. Non-Maxwellian EDFs [expressed in terms of electron energy probability function (EEPf)] in (a) capacitive¹¹ and (b) inductive¹⁰ rf plasmas in argon at different gas pressures. Vertical lines in (b) correspond to plasma potential. At 100 and 300 mTorr, the EDF is Maxwellian for $\varepsilon < \varepsilon^*$ and ε_i , but it is not measured at $\varepsilon > \varepsilon_i$ where due to inelastic collisions, the EDF should be depleted. Reproduced with permission from Godyak, IEEE Trans. Plasma Sci. **34**, 755 (2006). Copyright 2006 IEEE and Godyak, Phys. Plasmas **12**, 055501 (2005). Copyright 2005 AIP Publishing LLC.

kinetic level, remains a great challenge for our understanding of electron kinetics and physics of gas discharges.

Finally, the formation of distinct groups of electrons in the cathode region of classical dc glow discharges and in rf capacitive and inductive discharges is also a distinct kinetic effect. The kinetic approach has been used to explain the nature of negative glow and Faraday dark space (FDS), and the origin of electric field reversals in the cathode region. The highly anisotropic runaway electrons formed in the cathode sheath are responsible for the negative glow, and the hollow cathode effect. The slow electrons trapped in the potential well due to the field reversals are responsible for the peak of plasma density in the Faraday dark space. It turned out that the formation of distinct electron groups is a common phenomenon for dc, rf capacitive, inductive discharges, and space plasma (solar wind).

Recently, attention of a substantial part of the gas discharge community has shifted from low-pressure plasma systems to atmospheric-pressure microdischarges. However, the importance of electron kinetic effects discovered in low-pressure plasmas has not vanished but reduced in the spatial scale. Striations, runaway electrons, fast ionization waves, and other phenomena have been experimentally observed in these systems (thanks to pd scaling). It became clear that the kinetic approach may have to be applied in the dynamically evolving streamer fronts or gas-liquid interfaces, which have to be resolved with high accuracy to understand the key physical phenomena. Since experimental studies are difficult or impossible at these scales, simulations should play an increasingly important role. Classical gas discharges at low gas pressures with their convenient spatial scale for the experimental studies, and scaling laws, should remain as valuable tools for modeling and experimental validation of computer codes in LTP science.

We present an overview of recent advances in the field of electron kinetics in LTP focusing in four areas: (1) nonlocal and nonlinear electrodynamics, (2) formation of distinct electron groups in gas discharges and space plasmas, (3) kinetics of fast runaway electrons, and (4) nonlocal and transient effects. The authors' views on where the field is headed and on promising strategies for progress are described.

II. NONLOCAL AND NONLINEAR ELECTRODYNAMICS

Thermal motion of electrons plays an essential role in discharge plasmas at low gas pressures, similar to collisionless space and fusion plasmas. The near-collisionless electron motion in spatially nonuniform rf electric fields is responsible for the anomalous skin effect, collisionless electron heating, and negative power absorption observed in experiments. The domain of nonlocal plasma electrodynamics is defined by the relation¹⁰

$$\Lambda = \frac{v_{th}^2}{\lambda_E^2(\nu^2 + \omega^2)} \geq 1, \quad (1)$$

where Λ is the nonlocality parameter, $\lambda_E = (dE/dr)^{-1}$ is the characteristic length of rf electric field $E(r)$ localization, $v_{th} = (T_e/m)^{1/2}$ is the electron thermal velocity, and ν is the electron-atom collision frequency.

When the condition described by Eq. (1) is satisfied, the electron mean free path is comparable to or larger than λ_E , and electrons spend a short time compared to the rf period in the region of spatially inhomogeneous field (skin layer). The thermal motion of electrons results

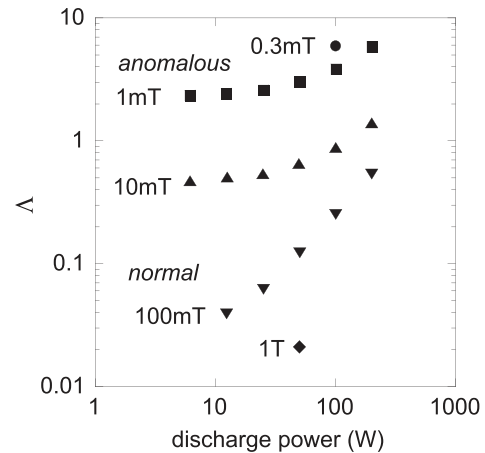


FIG. 2. Nonlocality parameter Λ for ICP driven at 6.8 MHz in argon gas. Reproduced with permission from Godyak, Phys. Plasmas **12**, 055501 (2005). Copyright 2005 AIP Publishing LLC.

in a spatial dispersion of the electron rf current, and the rf current density $\mathbf{j}(\mathbf{r})$ becomes a nonlocal function of the rf electric field $\mathbf{E}(\mathbf{r})$. The Ohm's law, $\mathbf{j} = \sigma_p \mathbf{E}$, becomes invalid. The nonlocal electrodynamics in LTP (which is essentially a hot plasma effect disappearing at $T_e \rightarrow 0$) is well known for CCP (where λ_E is the length of the rf sheath) and in ICP (where λ_E is the skin depth). The nonlocality parameter Λ calculated for ICP is shown in Fig. 2 for different argon pressures and rf powers. At $\Lambda \ll 1$, the ICP is in the regime of a normal skin effect, and can be adequately described by the conductivity of cold plasma σ_p . At $\Lambda \gg 1$, the ICP is in the regime of strong electrodynamic nonlocality (i.e., strong anomalous skin effect). Examples of nonlocal electrodynamics effects, collisionless electron heating, and negative power absorption are shown in Figs. 3 and 4.

External magnetic fields as weak as 3 G can drastically change the properties of low pressure ICPs.²¹ Effects of static magnetic fields are

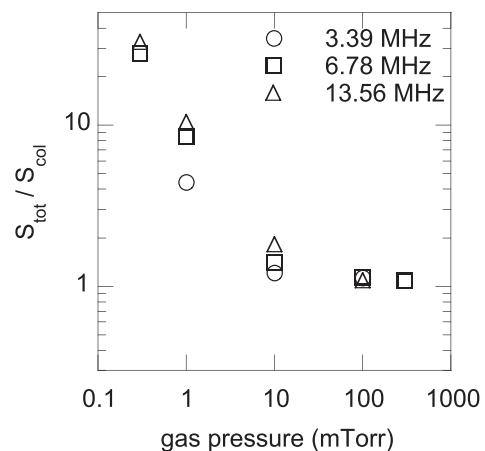


FIG. 3. The ratio of the measured total power absorption to calculated collisional power absorption in argon ICP. Reproduced with permission from Godyak, Phys. Plasmas **12**, 055501 (2005). Copyright 2005 AIP Publishing LLC.

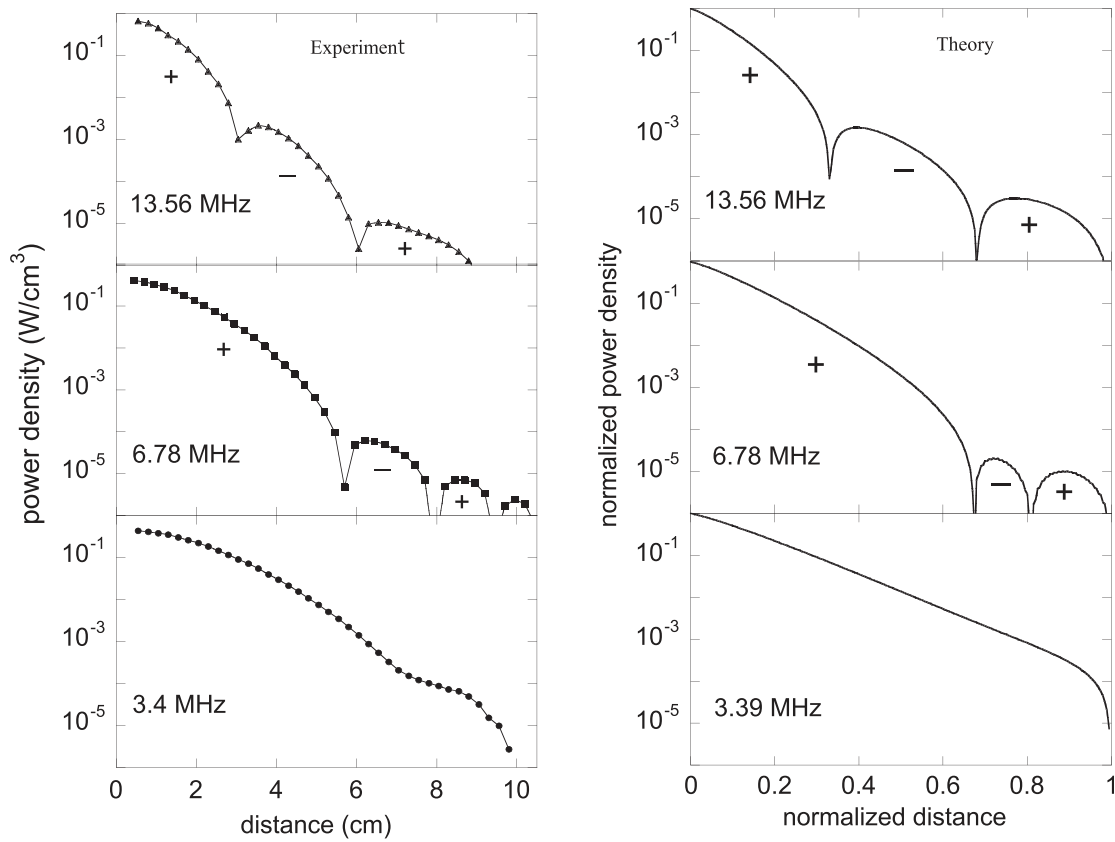


FIG. 4. Negative power absorption in argon ICP at 10 mTorr. Reproduced with permission from Godyak, *Phys. Plasmas* **12**, 055501 (2005). Copyright 2005 AIP Publishing LLC.

most pronounced when the nonlocality parameter Λ has a minimum. In cylindrical “ring” discharges with a spiral coil, application of weak static magnetic field parallel to the plasma boundary changes the radial profile of the rf magnetic field, when the electron Larmor radius becomes comparable to the tube radius. When the static magnetic field is perpendicular to the plasma boundary (as in ICP with planar coils), weak magnetic fields of only a few Gauss completely modify the nature of the rf field penetration into plasma.^{22,23} The observed enhanced penetration of the rf magnetic fields into plasma is due to electron cyclotron resonance and excitation of helicon waves.^{24–26}

Electrodynamic nonlocality ($\Lambda > 1$) is expected to occur in other rf and microwave plasmas produced in helicon,²⁷ surface wave, and microwave discharges, provided the condition (1) is satisfied. But theories and numerical models for these discharges still often use cold plasma (local electrodynamics) approximation. Helicon waves in bounded plasma correspond to whistler waves in free space.²⁸ Electron interactions with whistler waves have been actively studied in space physics for solar wind and aurora electrons.^{29,30}

The electric field responsible for ICP maintenance is generated by a time-varying magnetic field. The amplitude of the electric field scales as $E \propto \omega B$. For typical ICP geometries, the rf magnetic field is present in plasma together with rf electric field. To satisfy the electron energy balance in ICP, approximately the same magnitude of rf electric field is required at different driving frequencies. Therefore, for ICP

operation at low frequency and low gas pressure, a significant rf magnetic field should be present in the skin layer. At such a large rf magnetic field, the Lorentz force $F_L \propto v_{\omega} \times B_{\omega}$ exceeds the electric force $F_E \propto E$ in the skin layer. The condition $F_L/F_E > 1$, which is equivalent to

$$\omega_c^2 > \omega^2 + \nu^2 \quad (2)$$

defines the domain of a nonlinear skin effect. Here, v_{ω} is the electron oscillatory velocity and ω_c is the electron cyclotron frequency corresponding to the rms value of B_{ω} . The ratios F_L/F_E for different driving frequencies and argon pressures are shown in Fig. 5.

A variety of nonlinear effects appear due to the rf magnetic field and the $v_{\omega} \times B_{\omega}$ Lorentz force within the skin layer. For example, the rf magnetic field forces the electron velocity kick to occur normal to the plasma boundary during collisionless electron motion within the skin layer. Plasma rf polarization on the second harmonic and second harmonic current was discovered in ICP at low driving frequency.¹⁰ The origin of the second harmonic current $J_{z,r2\omega}$ and its radial distribution are shown in Fig. 6. Since the value of $J_{z,r2\omega}$ is comparable to the main discharge azimuthal current $J_{\theta\omega}$ at the fundamental frequency, $J_{z,r2\omega}$ may contribute to the electron energy balance in ICP.

At low driving frequency and low gas pressure [under condition (2)], the ponderomotive (Miller) force $F_p \propto \nabla E^2$ (i.e., the time averaged Lorentz force) can considerably affect the plasma density profile¹⁰ and modify the EDF in the skin layer.¹⁹ The experimentally observed

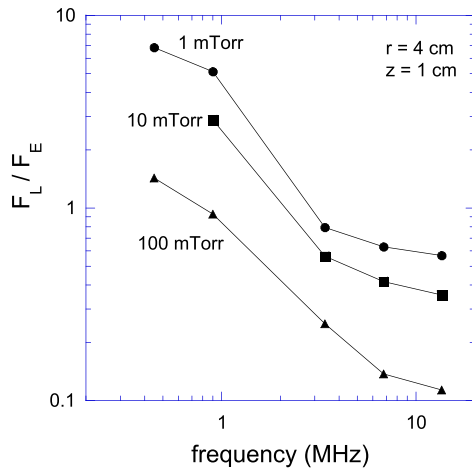


FIG. 5. The F_L/F_E ratio measured in the ICP skin layer. Reproduced with permission from Godyak, Phys. Plasmas **12**, 055501 (2005). Copyright 2005 AIP Publishing LLC.

EDF was depleted with the low energy electrons, which experienced larger ponderomotive force than the high energy electrons, and thus were pushed out of the skin layer.¹⁹

The axial plasma density, $n(0, z)$, and negative potential distributions, $V_p(0, z)$, measured at the ICP axis ($r=0$) and that at $r=4$ cm (within the maximum of the rf electric field and discharge current) are shown in Fig. 7. In accordance with the Boltzmann relation, $n = n_m \exp\left(-\frac{eV_p}{T_e}\right)$, the axial position of the maximal plasma density n_m (at $r=0$, $z=3.5$ cm where $F_L=0$) coincides with the position of the minimal potential $V_p=0$, while at $r=4$ cm, these positions diverge. This violation of the Boltzmann relation is attributed to the ponderomotive force, $F_p = en \nabla U_p$, and is well explained by the following force equilibrium equation: $T_e \nabla n + en \nabla V_p + en \nabla U_p = 0$, where U_p is the ponderomotive potential.

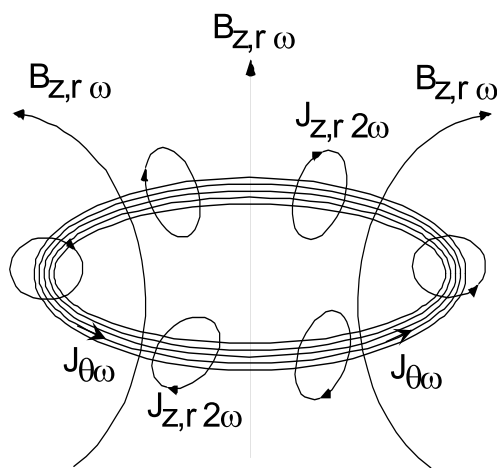


FIG. 6. The origin of the second harmonic current in ICP and its radial distribution. Reproduced with permission from Godyak, Phys. Plasmas **12**, 055501 (2005). Copyright 2005 AIP Publishing LLC.

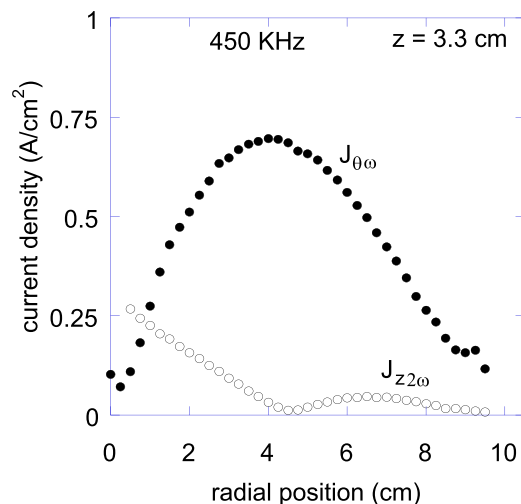
The values of the plasma potential V_p and thermopotential $T_p = T_e \ln(n_m/n)$ are shown in Fig. 8 for two radial positions. They coincide at $r=0$ since there $E_\theta, F_L, F_p = 0$; thus, the Boltzmann equilibrium ($T_p = V_p$) is held. In the area of strong electric field (at $r=4$ cm), the difference of $T_p - V_p = U_p$ allows one to find the ponderomotive force and its potential.

It is interesting that the experimentally observed ponderomotive force in ICP appears to be almost an order of magnitude smaller than the one predicted by the classical expression for the Miller force using cold plasma approximation. The discrepancy was resolved by the theory taking into account the electron thermal motion.³¹ Ironically, the Miller expression for the ponderomotive force applicable for hot fusion plasma fails in cold ICPs. The explanation of this paradox is due to the disparity of driving frequencies used for hot plasma and for ICP (gigahertz vs megahertz). Condition (2) is not satisfied in the first case. "Note that many outlined above features of the anomalous and nonlinear skin effect are ignored in all known numerical codes for plasma processing and ion sources."

III. FORMATION OF DISTINCT ELECTRON GROUPS IN GAS DISCHARGES AND SPACE PLASMAS

The formation of distinct groups of electrons is a common phenomenon in gas discharge plasma. It is now well explained by the kinetic theory of gas discharges that electrons with different energies can behave quite independently of each other, provided the Coulomb interactions are too weak to Maxwellize the EDF (that is the case for practically all LTPs). As a result, fluxes of electrons with different energies can flow in different directions with respect to gradients of plasma density and electric field direction.^{2,3}

Figure 9 illustrates the formation of three groups of electrons in the cathode region of classical dc glow discharges.² The first group of electrons consists of highly anisotropic runaway electrons formed in the cathode sheath, which are responsible for the nonlocal ionization in negative glow, and the peculiar properties of glow discharges with electrostatic confinement of fast electrons.³² The second group consists



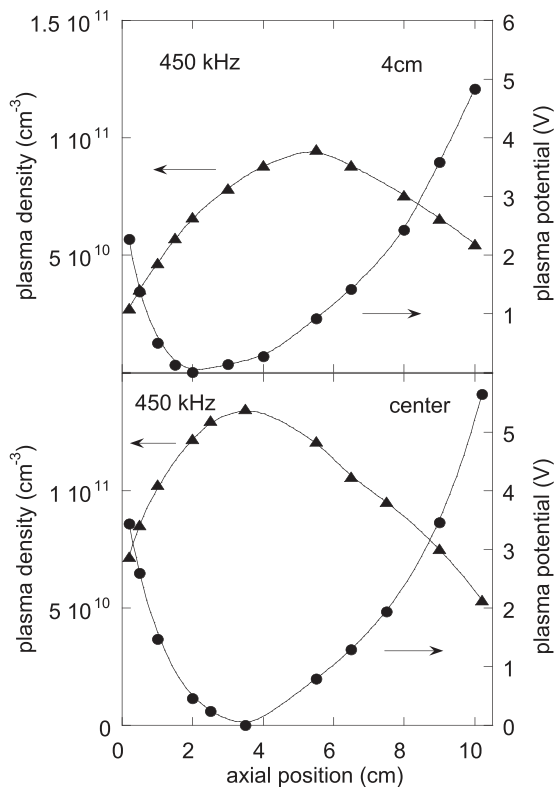


FIG. 7. Axial distribution of plasma density and plasma electrical potential in ICP. Reproduced with permission from Godyak, *Phys. Plasmas* **12**, 055501 (2005). Copyright 2005 AIP Publishing LLC.

of slow electrons trapped in the potential well formed in the cathode region due to the two field reversals. The slow electrons are responsible for the peak of plasma density in the Faraday dark space (FDS), but give zero contribution to the electron current transported by the third group of intermediate electrons, which consists of the decelerated fast electrons and the new electrons generated in the negative glow (NG). The intermediate electrons have near-isotropic velocity distribution. Their nonlocal kinetics can sometimes produce standing striations in the transition between the FDS and positive column. It turned out that the formation of distinct electron groups is a common phenomenon for dc, rf capacitive, inductive discharges, and space plasma (solar wind).

It is remarkable how the formation of three electron groups in the cathode region resembles the formation of three electron groups in solar wind. Stars and planets lose atmosphere because fast particles can overcome gravitational force and escape. Kinetics of escaping neutral and charged particles depends on the presence of magnetic fields. Sun has strong magnetic field to magnetize both electrons and ions in the entire heliosphere. Velocity distributions of electrons in solar wind exhibit three groups: core, halo, and strahl (see Fig. 10). The isotropic Maxwellian “core” comprises the bulk of the electron density. A magnetic-field-aligned beam (from ~50 eV to 1 keV) is called “strahl,” and a nearly isotropic component is called “halo.” Strahl formation is a result of kinetic beam focusing in spatially weakening magnetic field and its broadening via electron pitch-angle scattering. The pitch-angle

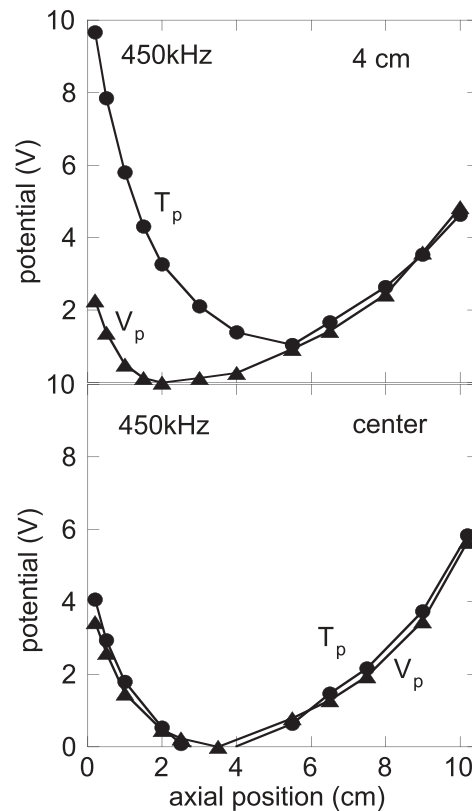


FIG. 8. Axial distribution of plasma electrical potential and plasma thermopotential in ICP. Reproduced with permission from Godyak, *Phys. Plasmas* **12**, 055501 (2005). Copyright 2005 AIP Publishing LLC.

scattering can be provided by Coulomb collisions between electrons and ions, or wave-particle interactions (such as whistler-mode turbulence). The relative contributions of Coulomb scattering and scattering via wave-particle interactions at different electron energies are a subject of active current studies. It has been recognized^{33,34} that the effect of spherical geometry on neutral particles is exactly equivalent to the

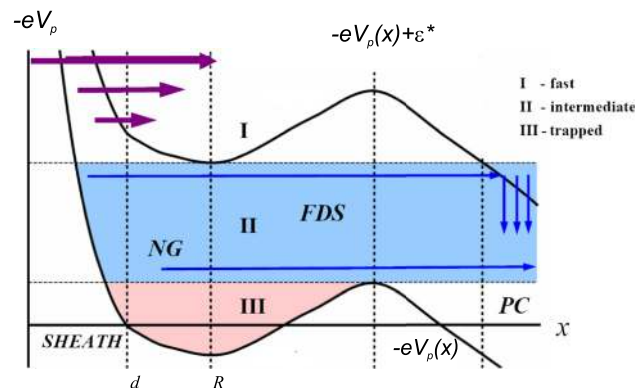


FIG. 9. Three groups of electrons in the cathode region of dc discharges. Dashed lines indicate the sheath-plasma boundary, two points of field reversals in plasma, and the boundary of the positive column.

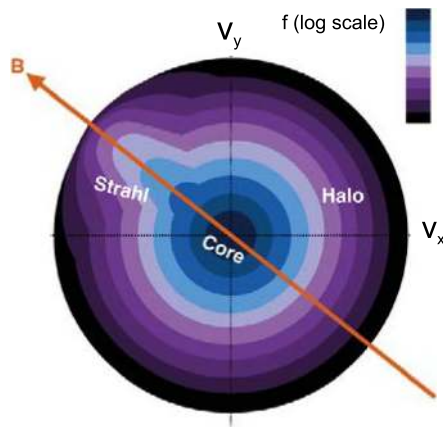


FIG. 10. An illustration of a typical velocity distribution of solar wind electrons. Reproduced with permission from Graham *et al.*, J. Geophys. Res. Space Phys. **122**, 3858 (2017). Copyright 2017 Author(s), licensed under a Creative Commons Attribution (CC BY) license.

effect of diverging magnetic field on magnetized charged particles. Scattering via Coulomb collisions counteracts magnetic focusing effects limiting the beam collimation by 24° for electrons with an energy of ~ 100 eV.³⁵

The halo is nearly isotropic, non-Maxwellian, and occupies the energy range ~ 70 – 1000 eV. Its angular distribution is formed due to pitch-angle scattering of strahl electrons by different mechanisms, and the energy distribution depends on the energy transfer in collisions and wave-particle interactions in a plasma-generated electric field.³⁶ This electric field is produced in expanding plasma to ensure quasi-neutrality. As a result, some of the electrons are trapped at the far end via electrostatic force and at the Sun side by the magnetic force. A reverse current toward the Sun should flow inside the halo to compensate for the current transported by the strahl electrons.

The formation of electron groups in solar wind resembles the formation of electron groups in the cathode region in several aspects. The electrons injected from the cathode and those generated in the cathode sheath form the group of fast electrons resembling the strahl. The slowest electrons, which are trapped in a potential well between the two field reversals, are similar to the core electrons, which constitute the majority of electrons in both cases. Finally, the nearly isotropic “intermediate” electrons are similar to the halo electrons. Indeed, the characteristic energies of the three electron groups in discharge plasma are different from those in solar wind. In solar wind, Coulomb interactions among charged particles and, possibly, wave-particle interactions are the main collisional processes. In gas discharges, elastic and inelastic collisions of electrons with neutrals and electron interactions with external electric fields are the key processes responsible for EDF formation. So the differences in energies are not surprising.

It is now well understood in the gas discharge physics that electrons with different energies can behave quite independently of each other. However, in space plasma, the kinetic approach appears less established. It was proposed that the observed maximum of temperature in the Sun corona is due to the velocity filtration effect, and there is no need for additional heat sources, as required by fluid models.^{37,38} However, the kinetic approach still appears as “a very interesting but

controversial idea: The heating necessary to produce the steep temperature inversion in the solar transition region and corona can be achieved without any wave or magnetic energy needing to be deposited” according to a recent paper,³⁹ which elaborates the same concept.

IV. FAST RUNAWAY ELECTRONS

Fast electrons with kinetic energies greatly exceeding the excitation and ionization thresholds of neutrals, and runaway electrons (RE) are commonly present in LTP. They appear in short-pulsed high-voltage discharges,⁴⁰ commonly generated in spatially inhomogeneous electric fields in the cathode sheath of dc discharges² and streamer fronts,⁴¹ and produced in the upper atmosphere by solar wind and cosmic rays.⁴²

If the energy of fast electrons exceeds the binding energy of all electrons in the target media, the interactions of fast electrons with the target can be considered using the Rutherford model for collisions among free charged particles.⁴³ Thus, deceleration of fast electrons in neutral gases can be described as a continuous slowing down by a retarding force given by the Bethe-Bloch law, and the momentum relaxation is dominated by small-angle scattering, and can be described as diffusion over pitch angle.

The kinetic equation for the fast electrons can be written in the form^{42,43}

$$\begin{aligned} \frac{\partial f}{\partial t} + v\mu \frac{\partial f}{\partial x} - \frac{eE}{m} \left(\mu \frac{\partial f}{\partial v} + \frac{1-\mu^2}{v} \frac{\partial f}{\partial \mu} \right) \\ = \frac{1}{v^2} \frac{\partial}{\partial v} (v^2 F f) + D_\mu \frac{\partial}{\partial \mu} \left((1-\mu^2) \frac{\partial f}{\partial \mu} \right) + I_e, \end{aligned} \quad (3)$$

where $\mu = \cos \theta$, and θ is the pitch angle, $F(v)$ is the dynamic friction, $D_\mu(v)$ is the diffusion coefficient, and I is a source term, which can include ionization events, or large angle scattering that cannot be described by the diffusion model. Kinetic equation (3) has been used for the description of runaway electrons in high electric fields, kinetics of solar wind electrons, precipitation of high-energy magnetospheric electrons into the ionosphere, degradation of fast electrons in the upper atmosphere, and other problems.

Kinetic equation (3) describes the formation of the EDF in a three-dimensional phase space: One spatial dimension and two-dimensional spherical velocity space. Modifications of this equation have been used for different problem types.⁴⁴ For electron energies close to the excitation threshold, the continuous slowing down approximation becomes invalid, and the loss function must be replaced by a sum of discrete collision cross sections. Forward scattering is often assumed for excitation or ionizing collisions because these collisions are much more forward peaked than elastic encounters. Furthermore, this approximation may continue to yield valid results at energies close to the first excitation threshold for the additional reason that the EDF becomes close to isotropic at these energies, in which case the angular dependence of the various scattering processes becomes unimportant.

Furthermore, kinetics of fast electrons has been described using a two-stream model or a forward-backward approximation, which were introduced (independently) for electron kinetics in the upper atmosphere,⁴⁵ fast electrons in gas discharges,^{46,47} and semiconductor transport.⁴⁸ The two-stream model assumes that electrons can move only along one spatial dimension with positive or negative velocities.

An example of simulating runaway electrons formed in a spatially inhomogeneous electric field with the two-stream model is

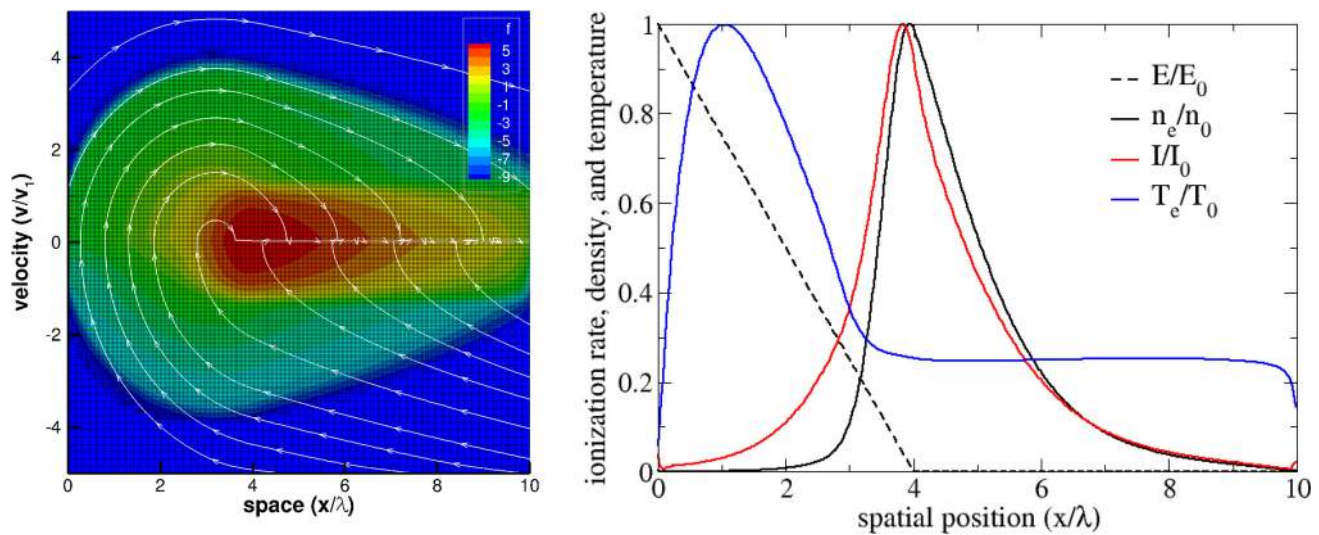


FIG. 11. Streamlines (characteristics), adapted computational mesh, and calculated EDF (color map in log scale) in the 1d1v phase space (left), and spatial distributions of normalized electric field E , electron density, ionization rate, and temperature (right).

shown in Fig. 11.⁴⁹ The model takes into account acceleration, scattering, energy loss in collisions, and electron-impact ionization for a linearly decreasing electric field near the cathode. The value of the electric field at the cathode surface ($x=0$) is high enough to guarantee the generation of runaway electrons at $eE(x)/F_0 > 1$, where F_0 is the maximum value of the loss function.^{2,3} The left part of Fig. 11 shows the calculated EDF with account for all the processes mentioned above. Electrons are injected at the left boundary ($x=0$), move along white stream lines, and get absorbed at the anode, at $x=L$. Elastic scatterings produce jumps between positive and negative values of v . Due to the decrease in the back-scattering rate with electron energy, there is an asymmetry between the positive and negative v : Slow

electrons have a near-isotropic EDF, whereas fast runaway electrons have a strongly anisotropic EDF. The right part of Fig. 11 shows the spatial distributions of the electric field, ionization rate, electron density, and temperature, which correspond to the typical distributions observed in the cathode region of short glow discharges without a positive column.^{2,3}

Extremely short (picosecond) pulses of runaway electrons (REs) are shown in Fig. 12 for a vacuum and atmospheric air. They were experimentally observed at the anode at the electric field rise rate of 10^{18} V/(cm s) and cathode-anode gap of 1 cm.⁵⁰ The electron current pulse in a vacuum is substantially lower in amplitude than that of REs in gas, and the RE current in gas arises earlier and has a duration of

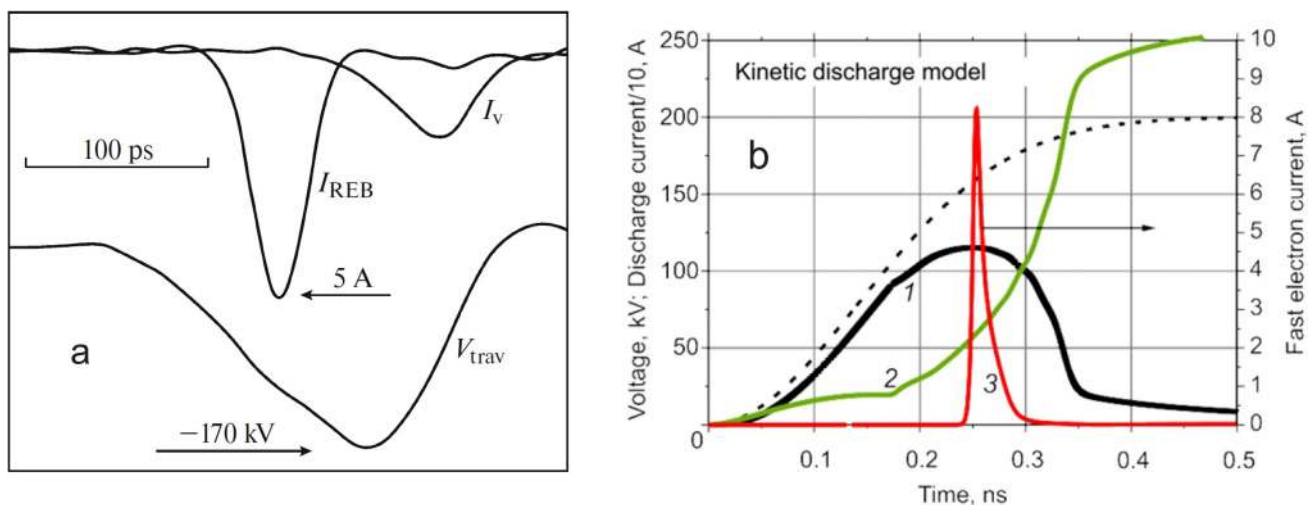


FIG. 12. The voltage pulse (U_v), the current from the cathode in vacuum (I_v), and the RE beam current in air (I_{REB}). (left) Reprinted with permission from Mesyats, Plasma Phys. Rep. 43, 952 (2017). Copyright 2017 Springer Nature. The source voltage (dashed curve), waveform of the voltage on cathode (curve 1), current in the circuit (curve 2), and the fast electron beam current (curve 3). (right) Reprinted with permission from Kozhevnikov *et al.*, Russ. Phys. J. 61, 603 (2018). Copyright 2018 Springer Nature.

~ 100 ps. The right part of Fig. 12 shows results of recent computational studies for similar conditions (nitrogen pressure of 760 Torr, interelectrode gap 1 cm, voltage pulse with amplitude of 200 kV and rise time of 200 ps). The model is based on solving the kinetic equation for electrons using the two-stream approximation with account for elastic scattering and ionization.⁵¹ The electric field is calculated self-consistently taking into account the displacement current and an external circuit. It is seen that the electron beam current pulse has a duration of about 15 ps, and the number of fast electrons in this beam pulse is about $\sim 10^9$. This result coincides qualitatively well with the experimental data shown in the left part of Fig. 12 and with other published results, both in the number of electrons per pulse and in the pulse duration.

Runaway electrons are expected to appear in front of fast ionization waves, streamer, and leader tips, during natural lightning and in high-voltage laboratory experiments.^{40,41} Direct sensor measurements of electric field inside the leaders or streamers are not possible even in the controlled laboratory discharges, due to too small spatial and temporal scales of the domains occupied by the field. The X- and γ -ray emissions are the only evidence that the electric field intensity is locally increased to the levels required for the RE generation. “To simulate these processes, the kinetic models described above must be further developed and applied inside dynamically evolving kinetic patches embedded into fluid plasma models.”

V. SPATIAL AND TEMPORAL SCALES AND DIFFERENT PLASMA MODELS

A. Three regimes of plasma operation

For the analysis of plasma dynamics, the most important factor is the distinction of electron and ion time scales. Due to the large differences of electron and ion time scales, one can distinguish three regimes of plasma operation: quasistatic (QS), dynamic, and high frequency.⁵² To illustrate key features of these regimes, consider discharges in noble gases at relatively low gas pressures, when the loss of charged particles is determined by surface recombination rather than volume recombination. In this case, the largest characteristic time scale is the time τ_a of ion transport to the wall. For a collisional plasma, the corresponding characteristic frequency ν_a is determined by the ambipolar diffusion, $\nu_a = D_a/\Lambda^2$, where Λ is the characteristic size of the plasma and D_a is the ambipolar diffusion coefficient. For nearly collisionless plasma, $\nu_a = v_s/\Lambda$ where v_s is the ion sound speed.

The three regimes mentioned above are distinguished based on the process time scale τ , the transport time scales $\tau_a = \nu_a^{-1}$, and the electron energy relaxation time τ_e , which is the second slowest time scale defined below.

Consider a discharge maintained by an electric field with frequency ω . The quasistatic regime corresponds to the low-frequency case ($\omega < \nu_a$) when plasma density varies significantly over the field period following the electric current. In this case, the electric field and electron temperature exhibit highly nonlinear behavior: They remain practically constant during the most part of the half-period and drop sharply near current zero (see the black curve in Fig. 13). At high frequencies ($\omega > \nu_e$) the electron energy distribution function (EEDF) (thus, the plasma density n and the electron temperature, T_e) is constant over period (as shown by the green curve in Fig. 13), and the electric field is: $E = E_0(1 + \omega^2/\nu_{eff}^2)^{1/2}$, where E_0 is the electric field in dc plasma at the same gas pressure and geometry, and ν_{eff} is the effective electron collision frequency accounting for collisional and stochastic electron heating. The field E_0 depends on the product $p\Lambda$, and adjusts itself according to electron energy balance.¹¹

The intermediate case ($\nu_a < \omega < \nu_e$) corresponds to a “dynamic regime.”^{52,53} In this regime, the plasma density varies slightly over the field period but the electron temperature, ionization rate, and the EEDF shape could change significantly over the field period. No detailed studies of this regime have been performed so far. A recent paper on low-frequency ICP⁵² is one step in this direction.

B. Different models for electron kinetics

In terms of electron kinetics, the key factor is that the momentum and energy relaxation processes occur at different spatial and temporal scales, which also depend on electron kinetic energy. For thermal electron energies, the momentum relaxation occurs faster than energy relaxation ($\tau_m \ll \tau_e$) and the electron mean free path λ_m is considerably smaller than its energy relaxation length λ_e . This situation, which is depicted schematically in Fig. 14, is opposite to the one taking place for the fast electrons described in Sec. IV.

In this figure, $\lambda = v_{ph}/\omega$ is the wavelength in plasma, v_{ph} is the phase velocity of electromagnetic field in plasma, and L is a characteristic spatial scale (device size). When the device size L is larger than λ , a full Maxwell solver should be used. At $L \ll \lambda$, the field is close to static (electrical/magnetic), and quasistatic (QS) models can be applied. Depending on characteristic spatial and temporal scales, different models can be applicable for the description of electron kinetics.

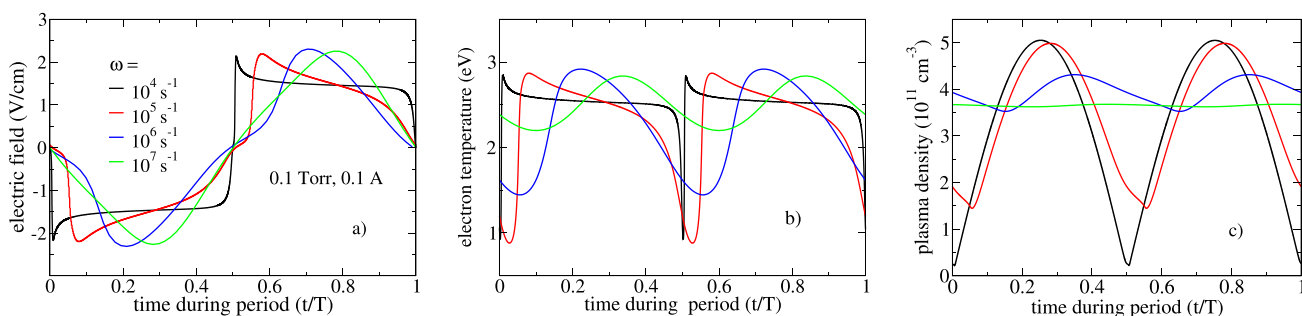


FIG. 13. Time dependence of the electric field (a), electron temperature (b), and plasma density (c) on axis of the tube for different frequencies at 0.1 Torr and 0.1 A. Reprinted with permission from V. I. Kolobov and V. A. Godyak, Plasma Sources Sci. Technol. **26**, 075013 (2017). Copyright 2017 IOP Publishing..

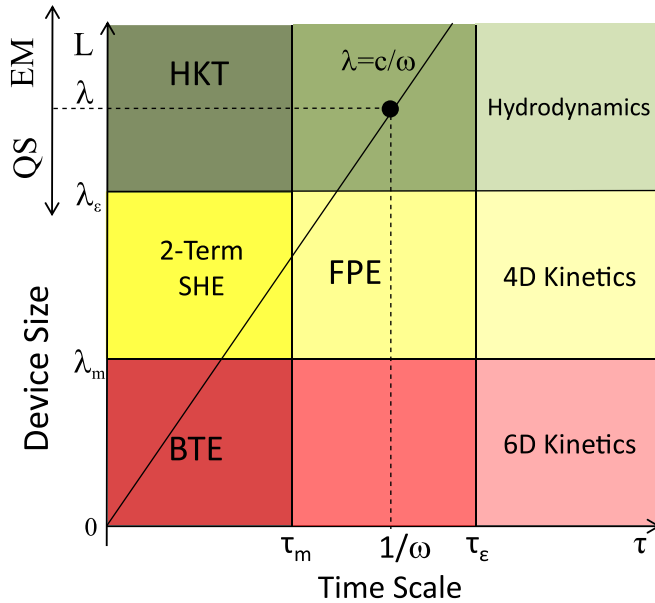


FIG. 14. Selection of physical models depending on the time scale and device size.

When spatial scales exceed the electron energy relaxation length λ_e , and the time scales exceed the energy relaxation time τ_e , the electron transport can be described by fluid models with EDFs depending on *local* electric fields. The transport coefficients (mobility and diffusion) of electrons can be calculated from the EDFs. This model is well established and has been widely used in the modeling of gas discharge plasmas.^{54,55}

At spatial scales exceeding the momentum relaxation length λ_m , and time scales exceeding the momentum relaxation time τ_m , the EDF is close to isotropic and can be described using the first two terms of the Spherical Harmonics Expansion (SHE) in velocity space⁵⁶

$$\frac{\partial f_0}{\partial t} + \frac{\mathbf{v}}{3} \cdot \nabla \cdot \mathbf{f}_1 + \frac{1}{3v} \frac{\partial}{\partial \varepsilon} (\mathbf{v} \cdot \mathbf{E} \cdot \mathbf{f}_1) + \frac{1}{v} \frac{\partial}{\partial \varepsilon} \left(\mathbf{v} \left[V_e(\mathbf{r}, U) f_0 + D_e(\mathbf{r}, U) \frac{\partial f_0}{\partial \varepsilon} \right] \right) = S_0, \quad (4)$$

$$\frac{\partial \mathbf{f}_1}{\partial t} + \boldsymbol{\omega}_c \times \mathbf{f}_1 + \nu_m \mathbf{f}_1 = -\mathbf{v} \left(\nabla f_0 - e \mathbf{E} \frac{\partial f_0}{\partial \varepsilon} \right), \quad (5)$$

where ν_m is the momentum relaxation frequency, $\boldsymbol{\omega}_c$ is the cyclotron frequency vector, ε is the electron kinetic energy, and $U = \varepsilon - eV_p(\mathbf{r})$ is the *total* electron energy. According to Eq. (4), the quasi-elastic processes (including Coulomb interactions among electrons) are described as diffusion and convection along the energy axis with coefficient D_e and V_e . Inelastic processes associated with large energy jumps are taken into account by the right-hand side, S_0 .

For Coulomb interactions among electrons, λ_m and λ_e are of the same order of magnitude and strongly decrease with decreasing electron energy. For molecular gases, λ_m and λ_e have large values at energies corresponding to excitation of rotational and vibrational states of molecules. Their values depend not only on electron energies but also on specific populations of rotational and vibrational states. Thus, high-fidelity calculations of the EDF in molecular gases require self-

consistent analysis of electron kinetics and vibrational kinetics of molecules.⁵⁷ Superlattice collisions with metastable atoms could also affect the EDF shape.⁵⁸

For the simulation of plasma dynamics at the energy relaxation time scale, it is convenient to use *total* electron energy $U = \varepsilon - eV_p(\mathbf{r})$ as an independent variable, where V_p is the plasma potential. Combined Eqs. (4) and (5) give a Fokker-Planck equation for the Electron Energy Distribution Function (EEDF)⁵⁹

$$\frac{\partial f_0}{\partial t} - \frac{1}{N} \frac{\partial}{\partial x_i} \left(N D^{ij} \frac{\partial f_0}{\partial x_j} \right)_U + \frac{1}{N} \frac{\partial}{\partial U} \left(N \left[V_e(\mathbf{r}, U) f_0 + D_e(\mathbf{r}, U) \frac{\partial f_0}{\partial U} \right] \right) = S_0, \quad (6)$$

where $D^{ij}(\varepsilon)$ is the diffusion tensor, which becomes a scalar, and $D = \nu \lambda_m / 3$, for nonmagnetized plasma. For semiconductor plasmas, the diffusion tensor is defined as constant energy averages of the group velocity $\mathbf{v}_g = \partial \varepsilon / \partial \mathbf{p}$ and the vector mean free path $\lambda(\mathbf{p})$.⁶⁰ The Fokker-Planck equation (6) in the energy-position space has been used for modeling electron kinetics in semiconductors with realistic band structures.^{61,62}

The total energy paradigm was independently developed in gas discharge physics,² semiconductor physics,⁶² and space science.⁶³ “Generalized Boltzmann law” for trapped electrons, kinetic resonances at spatial scales $\sim \lambda_e = \varepsilon^* / (eE_0)$ (where ε^* is the first excitation threshold of atoms) in electric fields E_0 , fluxes of electrons with different total energies flowing in opposite directions—these are just a few examples of interesting nonlocal kinetic effects that have been observed and predicted in gas discharges using this paradigm.^{2,64} Under certain conditions, the EDF body is cooled by the ambipolar field, whereas its tail is heated by it.⁶⁵ This phenomenon cannot be explained in any way within the framework of the traditional hydrodynamic description, in which all electrons are heated or cooled by the field. In fully ionized plasma, due to strong dependence of the electron mean free path on kinetic energy, kinetic regimes for thermal and superthermal electrons can be quite different.⁶⁵ Heat flux transported by superthermal electrons is not proportional to the temperature gradient.

At spatial scales smaller than or comparable to the momentum relaxation length and for the time scales smaller than the momentum relaxation times, a full Boltzmann solver must be used. Furthermore, in molecular gases and semiconductors, the energy relaxation length may be comparable to the momentum relaxation length under certain conditions. Under these conditions, electron streaming can be observed in a certain range of electric fields. Under streaming conditions, the EDF is highly anisotropic, and the two-term SHE is not applicable.

C. Peculiarities of high-pressure microdischarges

Both low-pressure lab-scale discharges and high-pressure microdischarges generate nonequilibrium LTP. However, their size and operation pressure differ by orders of magnitude. Figure 15 compares key parameters of electron kinetics in noble gases for a conventional low-pressure discharge and an atmospheric pressure microdischarge.⁶⁶ At atmospheric pressure, the electron-neutral collision frequency ν_m is much larger than the rf driving frequency ω [Figs. 15(a) and 15(b)]. Therefore, the bulk plasma is mainly resistive, and the inductive

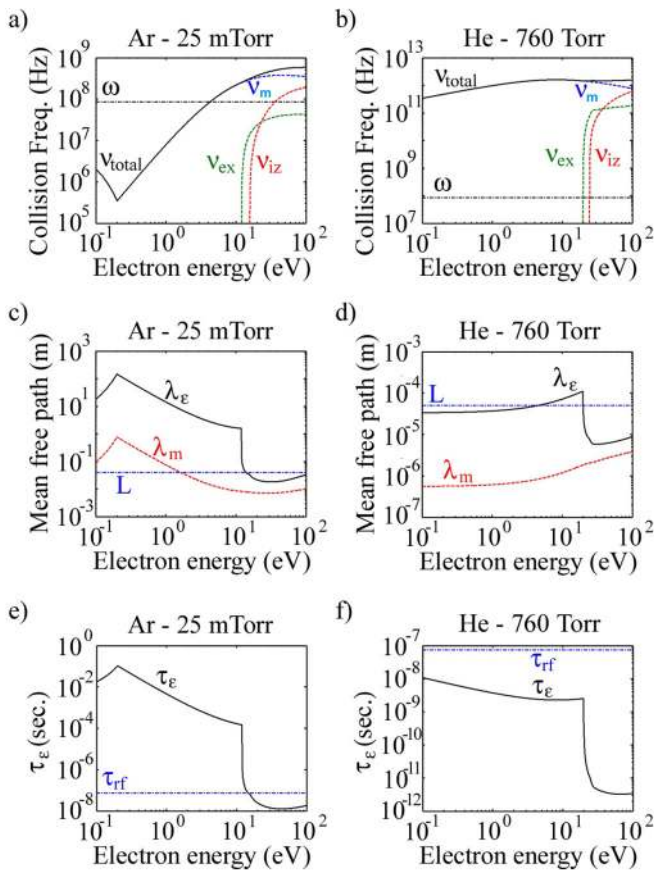


FIG. 15. Comparison between a low-pressure Ar discharge [(a), (c), and (e)] and an atmospheric-pressure He microplasma driven at 13.56 MHz [(b), (d), and (f)]: the electron-neutral collision frequencies (ν_{total} , ν_m , ν_{ex} , ν_{iz}) and the rf driving frequency ω [(a) and (b)]; the electron mean free path λ_m , the electron energy relaxation length λ_e , and the characteristic length of the system L ; the electron energy relaxation time τ_e and the rf period τ_{rf} [(e) and (f)]. Reprinted with permission from Iza *et al.*, *Plasma Processes Polym.* **5**, 322 (2008). Copyright 2008 John Wiley and Sons.

behavior due to the electron inertia often encountered in low-pressure discharges can be ignored ($\nu_m \gg \omega$ and $\sigma \approx \sigma_{\text{DC}}$). Furthermore, while the electron thermal velocity v_{th} is comparable in the two cases, the product of collision frequency times discharge size $\nu_m L$ is typically 100 times larger in microdischarges. As a result, the condition $\nu_m L \gg v_{\text{th}}$ is normally satisfied in microplasmas, so the collisionless electron heating is negligible, and the Ohmic heating with $\sigma_p = e^2 n / (m \nu_m)$ is the dominant heating mechanism.

It is normally accepted that nonlocal electron kinetics is important for low-pressure discharges, while local kinetics (and fluid models) is valid at higher pressure. However, it is erroneous to assume that in microdischarges the electrons are in local equilibrium with the electric field simply because the discharge operates at atmospheric pressure. In fact, the large electric fields and the reduced dimensions encountered in microdischarges contribute to a departure from the local kinetics. The transition from the local to the nonlocal regime takes place when the electron energy relaxation length becomes

comparable to the length of the spatial inhomogeneity of the electric field. In low-pressure plasmas, this length is approximately the size of the discharge gap, and electrons are found in the local or the nonlocal regime depending on the discharge conditions. For the 25 mTorr (3.3 Pa) Ar discharge used as an example in Fig. 15(c), low-energy electrons are in the nonlocal regime ($\lambda_e > L$), whereas high-energy electrons are marginally in the local regime ($\lambda_e < L$). The distinction between low- and high energy electrons is made because of the much faster collisional energy loss of electrons with energy above the inelastic (excitation) threshold. If the system length (L) in Fig. 15(c) had been 1 cm instead of 4 cm, all the electrons would be in the nonlocal regime.

Similarly, low-energy electrons in an atmospheric pressure microdischarge [Fig. 15(d)] may not be in local equilibrium with the electric field ($\lambda_e > L$). Indeed, nonlocal effects such as striations have been observed in high pressure microdischarges and linked to the nonlocality of low-energy electrons. The energy relaxation length (λ_e) of electrons in the elastic energy range ($e < 20$ eV for He) is $\sim 50 \mu\text{m}$ [Fig. 15(d)], which is of the same order as the width of the potential well experienced by low-energy electrons in a $100 \mu\text{m}$ discharge.

Unlike in low-pressure discharges, the electron energy relaxation time in an atmospheric microdischarge ($\tau_e \approx 5$ ps to 10 ns) is shorter than the rf period ($\tau \sim 74$ ns) [Figs. 15(e) and 15(f)]. As a result, the EDF is strongly modulated by the driving frequency, especially in the inelastic energy range. Because of this fast energy relaxation time, even rf capacitively coupled discharges at atmospheric pressure can be seen as a succession of dc discharges sustained at different voltages.

VI. THE PROMISING STRATEGIES FOR PROGRESS

A. Synergy between research studies in neighboring fields

Many fundamental properties of LTPs in gas discharges, space science, near-Earth environment, atmospheric electricity, and semiconductor physics are remarkably similar. Yet, researchers are often unaware about progress in their neighboring fields. We have mentioned several examples, such as independent discovery of the total energy benefits in gas discharges, semiconductor transport, space science, and the formation of different electron groups in gas discharges and solar wind plasma. Borrowing achievements from neighboring field can be very fruitful for future progress.

For example, the nonlocal electrodynamic and nonlinear kinetic effects found in gas discharges can also be important for terahertz technologies and surface wave effects in metals (plasmonics). Indeed, the skin depth reaches 200 nm at 100 GHz in copper, which is about 5 times the electron mean free path at room temperature. Size effects become a serious problem in on-chip interconnects. Superanomalous skin effects have been reported for surface plasmon polaritons.⁶⁷ How the plasma properties change when electrons undergo transition from magnetized to demagnetized in spatially nonuniform or time-varying magnetic fields? Can the accumulated gas discharge experience with convenient temporal and spatial scales be applied to terahertz science, magnetodynamics,⁶⁸ and plasmonics, where spatially resolved measurements are difficult or impossible due to limitations of time and space scales?

The second example concerns fast electrons. Fast electrons with kinetic energies greatly exceeding the excitation and ionization thresholds of neutrals are commonly present in LTPs. They appear in

short-pulsed high-voltage discharges, commonly generated in spatially inhomogeneous electric fields in the cathode sheath of dc discharges, in front of fast ionization waves, streamer, and leader tips, and produced in the upper atmosphere by solar wind and cosmic rays. Fast runaway electrons are responsible for the X- and γ -ray emissions observed in natural lightning and high-voltage laboratory experiments.⁴¹ Direct measurements of electric field inside the leaders or streamers are difficult or impossible even in the controlled laboratory discharges, due to too small spatial and temporal scales of the domains occupied by the field. The X- and γ -ray emissions are the only evidence that the electric field intensity is locally increased to the levels required for the RE generation. To simulate these processes, kinetic models must be further developed and applied inside dynamically evolving kinetic patches embedded into fluid plasma models.

There are two scientific communities, the ionospheric and magnetospheric, which deal with the theoretical description of diffuse auroral electron precipitation and its consequences. The ionospheric community focuses on superthermal electron transport at ionospheric altitudes without taking into account the magnetically conjugate region. The magnetospheric community focuses mostly on the processes that drive electron precipitation in the diffuse auroral region. The majority of the electron precipitation studies in the ionospheric and magnetospheric communities have been historically disconnected. The formation of the EDF at the ionosphere-magnetospheric boundary via ionosphere-magnetosphere coupling connects space science with collisional discharge physics.⁴² Studies of runaway electrons in gas discharges, electric discharges in the stratosphere and mesosphere (elves, sprites and jets), and lightning initiation and thunderstorm activity in the troposphere can benefit from collaboration of scientists working in these diverse fields.

As the third example, it has been recently shown⁵² that depending on geometry and the presence of ferromagnetic materials, the rf magnetic field may be completely absent in ICPs. Electron kinetics in magnetic-field-free ICPs has not been studied so far. Particularly interesting is that such systems can operate at very low frequencies, down to 50 Hz. Studies of electron kinetics at different frequencies including dynamic regimes could uncover interesting effects. In particular, strong electron magnetization by alternating magnetic field and demagnetization during the zero-B point should be associated with a strong heating effect that has not been studied so far. Demagnetization is a hot topic in space science in relation to magnetic reconnection.

As physics of LTPs becomes increasingly multidisciplinary, and includes processes at gas-liquid-solid interfaces, phase transitions, and extreme states of matter, the need for closer interactions of scientists from different areas of physics, chemistry, electrophysics, multiphase flow science, and even experts from physical and life sciences becomes important.

A. Strategies for progress with experiments

In terms of experiments, the biggest concern is a flow of unprofessional, low quality publications with violation of vacuum hygiene, ignorance of applicability and limitation of diagnostics used, and uncertainty of discharge conditions. Let us look at just a few typical examples. It is widely recognized that meaningful application of Langmuir probes in rf plasmas requires mitigation of rf voltage across the probe sheath, i.e., $V_{\text{srf}} < T_e/3e$, where V_{srf} is the rf voltage across the probe sheath and T_e is the electron temperature in eV. In order to

determine, whether this requirement is satisfied one has to measure the plasma rf potential V_{prf} to make an adequate rf filter with certain impedance characteristics. There is no measurement of V_{prf} and filter parameters in the majority of published studies on rf plasma diagnostics. Using just some filter does not mean that the probe is rf compensated and plasma parameters inferred from such measurement are valid. In the majority of publications, the authors report the rf power consumed from rf power source P_g . In fact, this power is higher (and sometimes considerably higher) and is not proportional to the power delivered to the plasma P_p . A significant portion of rf power dissipates in the matcher, induction coil, and (due to eddy current) in the metal chamber. Therefore, the power consumed by plasma P_p , which is the relevant parameter defining plasma condition, has to be evaluated and used in numerical simulation instead of the output power of rf generator P_g measured in the majority of experiments and used in simulation as the plasma power P_p .

In a positive sense, we see the challenge for the LTP experiment in the refining of the Langmuir-Druyvestein probe technique as the most informative for LTP diagnostics in the following directions: (a) plasma in magnetic field, (b) elevated gas pressures, (c) anisotropic plasma, and (d) fast transient and unstable plasmas. In recent years, considerable attention has been paid to probe diagnostics beyond the applicability of the classical Langmuir probe technique for these plasma conditions.^{69–74} Comprehensive testing and validation are required for the new methods with clear understanding of their applicability and limitations to be routinely applicable in plasma diagnostics.

B. Key areas where experiment and theory collaborations can help to facilitate scientific discoveries

Conditions of nonlocal and nonlinear electrodynamics found in laboratory CCP and ICP systems occur in commercial plasma sources of different types (including helicon, surface wave, etc.) as well as in metal plasmas (plasmonics). Therefore, elaboration of nonlocal and nonlinear electrodynamics effects into numerical plasma codes for those plasmas would be awarded with more realistic perception and understanding of these systems. In particular, we suggest the following key areas of research:

Designation of benchmark experiments with contemporary reliable diagnostics for testing and evaluation of numerical codes, similar to Gaseous Electronics Conference (GEC) Reference Cell, but with professionally designed chambers suitable for diagnostics is needed. Such experiments are extremely difficult and sometime impossible in industrial plasma sources hardly attainable for diagnostics. There is no need for many of such facilities (setups), one would be enough with close collaboration of many research groups of experimentalists, theorists, and numerical modelers (virtual experimentalists).

The study of feasibility and limitations of plasma diagnostics is performed using Langmuir, magnetic, and microwave probes for plasmas at elevated gas pressures, high magnetic fields, strong anisotropy of the VDF, and fast transient processes. Recent advances in simulations of particle kinetics for solid theoretical background of these diagnostics for real non-Maxwellian plasmas are applies.^{75,76}

Exploration of feasibility and limitations, and development of methods for plasma control (electron temperature and plasma density profile) to enhance efficiency of industrial plasmas are carried out. So far, in industry, plasma control is based on intuition and a “trial and

error” approach whereas numerical modeling remains not “predictive,” but rather confirming and sometimes only decorative. To be predictable, numerical modeling should generate scaling laws that are more valuable for plasma system design than low-informative color pictures for selected sets of external parameters.

ACKNOWLEDGMENTS

This work was partially supported by the U.S. Department of Energy Office of Fusion Energy Science Contract No. DE-SC0001939 and by the NSF EPSCoR Project No. OIA-1655280 “Connecting the Plasma Universe to Plasma Technology in AL: The Science and Technology of Low-Temperature Plasma.”

REFERENCES

- ¹F. Taccogna and G. Dilecce, “Non-equilibrium in low-temperature plasmas,” *Eur. Phys. J. D* **70**, 251 (2016).
- ²L. D. Tsendin, “Nonlocal electron kinetics in gas-discharge plasma,” *Phys. Usp.* **53**, 133 (2010).
- ³V. I. Kolobov, “Advances in electron kinetics and theory of gas discharges,” *Phys. Plasmas* **20**, 101610 (2013).
- ⁴S. Longo, “Monte Carlo simulation of charged species kinetics in weakly ionized gases,” *Plasma Sources Sci. Technol.* **15**, S181–S188 (2006).
- ⁵Z. Donko, “Particle simulation methods for studies of low-pressure plasma sources,” *Plasma Sources Sci. Technol.* **20**, 024001 (2011).
- ⁶R. R. Arslanbekov, V. I. Kolobov, and A. A. Frolova, “Kinetic solvers with adaptive mesh in phase space,” *Phys. Rev. E* **88**, 063301 (2013).
- ⁷M. Palmroth, U. Ganse, Y. Pfau-Kempf, M. Battarbee, L. Turc, T. Brito, M. Grandin, S. Hoilijoki, A. Sandroos, and S. von Alfthan, “Vlasov methods in space physics and astrophysics,” *Living Rev. Comput. Astrophys.* **4**, 1 (2018).
- ⁸V. I. Kolobov and R. R. Arslanbekov, “Towards adaptive kinetic-fluid simulations of weakly ionized plasmas,” *J. Comput. Phys.* **231**, 839 (2012).
- ⁹V. I. Kolobov and F. Deluzet, “Adaptive kinetic-fluid models for plasma simulations on modern computer systems,” *Front. Phys.* **7**, 78 (2019).
- ¹⁰V. A. Godyak, “Hot plasma effects in gas discharge plasma,” *Phys. Plasmas* **12**, 055501 (2005).
- ¹¹V. A. Godyak, “Non-equilibrium EEDF in gas discharge plasmas,” *IEEE Trans. Plasma Sci.* **34**, 755 (2006).
- ¹²V. Godyak and R. Piejak, “Paradoxical spatial distribution of the electron temperature in a low pressure rf discharge,” *Appl. Phys. Lett.* **63**, 3137 (1993).
- ¹³V. Godyak and B. Alexandrovich, “Langmuir paradox revisited,” *Plasma Sources Sci. Technol.* **24**, 052001 (2015).
- ¹⁴M. M. Turner, “Collisionless electron heating in an inductively coupled discharge,” *Phys. Rev. Lett.* **71**, 1844 (1993).
- ¹⁵M. A. Lieberman and V. A. Godyak, “From Fermi acceleration to collisionless discharge heating,” *IEEE Trans. Plasma Sci.* **26**, 955 (1998).
- ¹⁶I. D. Kaganovich, “Effects of collisions and particle trapping on collisionless heating,” *Phys. Rev. Lett.* **82**, 327 (1999).
- ¹⁷I. D. Kaganovich, O. V. Polomarov, and C. E. Theodosiou, “Landau damping and anomalous skin effect in low-pressure gas discharges: Self-consistent treatment of collisionless heating,” *Phys. Plasmas* **11**, 2399 (2004).
- ¹⁸M. M. Turner, “Collisionless heating in radio-frequency discharges: A review,” *J. Phys. D: Appl. Phys.* **42**, 194008 (2009).
- ¹⁹V. Godyak, B. Alexandrovich, and V. Kolobov, “Lorentz force effects on the electron energy distribution in inductively coupled plasmas,” *Phys. Rev. E* **64**, 026406 (2001).
- ²⁰V. I. Kolobov, “Striations in rare gas plasmas,” *J. Phys. D: Appl. Phys.* **39**, R487 (2006).
- ²¹V. I. Kolobov, “The anomalous skin effect in bounded systems,” in *Electron Kinetics and Applications of Glow Discharges*, NATO ASI Series B 367, edited by U. Kortshagen and L. D. Tsendin (Plenum Press, NY, 1998).
- ²²H.-J. Lee, I.-D. Yang, and K.-W. Whang, “The effects of magnetic fields on a planar inductively coupled argon plasma,” *Plasma Sources Sci. Technol.* **5**, 383 (1996).
- ²³V. A. Godyak and B. M. Alexandrovich, “Radio frequency potential of inductive plasma immersed in a weak magnetic field,” *Appl. Phys. Lett.* **84**, 1468 (2004).
- ²⁴C. Chung, S. S. Kim, and H. Y. Chang, “Electron cyclotron resonance in a weakly magnetized radio-frequency inductive discharge,” *Phys. Rev. Lett.* **88**, 095002 (2002).
- ²⁵C. W. Chung, S. S. Kim, and H. Y. Chang, “Experimental measurement of the electron energy distribution function in the radio frequency electron cyclotron resonance inductive discharge,” *Phys. Rev. E* **69**, 016406 (2004).
- ²⁶M.-H. Lee and S. W. Choi, “Evolution of an electron energy distribution function in a weak dc magnetic field in solenoidal inductive plasma,” *J. Appl. Phys.* **104**, 113303 (2008).
- ²⁷S. Isayama, S. Shinohara, and T. Hada, “Review of helicon high-density plasma: Production mechanism and plasma/wave characteristics,” *Plasma Fusion Res.* **13**, 1101014 (2018).
- ²⁸R. L. Stenzel, “Whistler waves with angular momentum in space and laboratory plasmas and their counterparts in free space,” *Adv. Phys. X* **1**, 687 (2016).
- ²⁹V. Pierrard, M. Lazar, and R. Schlickeiser, “Evolution of the electron distribution function in the whistler wave turbulence of the solar wind,” *Sol. Phys.* **269**, 421 (2011).
- ³⁰G. V. Khazanov, A. K. Tripathi, D. Sibeck, E. Himwich, A. Gloer, and R. P. Singhal, “Electron distribution function formation in regions of diffuse aurora,” *J. Geophys. Res. Space Phys.* **120**, 9891, <https://doi.org/10.1002/2015JA021728> (2015).
- ³¹A. Smolyakov, V. Godyak, and Y. Tyshetskiy, “Effect of the electron thermal motion on the ponderomotive force in inductive plasma,” *Phys. Plasma* **8**, 3857 (2001).
- ³²V. I. Kolobov and A. S. Metel, “Glow discharges with electrostatic confinement of fast electrons,” *J. Phys. D: Appl. Phys.* **48**, 233001 (2015).
- ³³Ø. Lie-Svendsen and M. H. Rees, “An improved kinetic model for the polar outflow of a minor ion,” *J. Geophys. Res.* **101**, 2415, <https://doi.org/10.1029/95JA02690> (1996).
- ³⁴Ø. Lie-Svendsen, V. H. Hansteen, and E. Leer, “Kinetic electrons in high-speed solar wind streams: Formation of high-energy tails,” *J. Geophys. Res.* **102**, 4701, <https://doi.org/10.1029/96JA03632> (1997).
- ³⁵K. Horaites, S. Boldyrev, and M. V. Medvedev, “Electron strahl and halo formation in the solar wind,” *Mon. Not. R. Astron. Soc.* **484**, 2474 (2019).
- ³⁶G. A. Graham, I. J. Rae, C. J. Owen, A. P. Walsh, C. S. Arridge, L. Gilbert, G. R. Lewis, G. H. Jones, C. Forsyth, A. J. Coates, and J. H. Waite, “The evolution of solar wind strahl with heliospheric distance,” *J. Geophys. Res. Space Phys.* **122**, 3858, <https://doi.org/10.1002/2016JA023656> (2017).
- ³⁷J. D. Scudder, “On the causes of temperature change in homogeneous low-density astrophysical plasmas,” *Astrophys. J.* **398**, 299 (1992).
- ³⁸J. D. Scudder, “Why all stars possess circumstellar temperature inversions,” *Astrophys. J.* **398**, 319 (1992).
- ³⁹V. Pierrard and M. Pieters, “Coronal heating and solar wind acceleration for electrons, protons, and minor ions obtained from kinetic models based on kappa distributions,” *J. Geophys. Res. Space Phys.* **119**, 9441, <https://doi.org/10.1002/2014JA020678> (2014).
- ⁴⁰L. P. Babich, *High-Energy Phenomena in Electric Discharges in Dense Gases* (Futurepast, 2003).
- ⁴¹L. P. Babich, E. I. Bochkov, I. M. Kutsyk, T. Neubert, and O. Chanrion, “Analyses of electron runaway in front of the negative streamer channel,” *J. Geophys. Res.: Space Phys.* **122**, 8974, <https://doi.org/10.1002/2017JA023917> (2017).
- ⁴²G. V. Khazanov, “Kinetic theory of the inner magnetospheric plasma,” in *Astrophysics and Space Science Library* (Springer, 2015), Vol. 372.
- ⁴³A. V. Gurevich and K. P. Zybin, “Runaway breakdown and electric discharges in thunderstorms,” *Phys. Usp.* **44**, 1119 (2001).
- ⁴⁴D. J. Strickland, D. L. Book, T. P. Coffey, and J. A. Fedder, “Transport equation technique for the deposition of auroral electrons,” *J. Geophys. Res.* **81**, 2755, <https://doi.org/10.1029/JA081i016p02755> (1976).
- ⁴⁵K. Stamnes, “On the two-stream approach to electron transport and thermalization,” *J. Geophys. Res.* **86**, 2405, <https://doi.org/10.1029/JA086iA04p02405> (1981).

- ⁴⁶Yu. P. Raizer and M. N. Shneider, "Simplified kinetic equation for electrons in nonuniform fields of arbitrary strength and cathode sheath of a glow discharge," *Sov. J. Plasma Phys.* **15**, 184 (1989).
- ⁴⁷L. P. Babich, K. I. Bakhov, I. M. Kutsyk, and B. N. Shamraev, "Method of simplified kinetic equation for simulating the electron kinetics in dense gases in strong electric fields," *Plasma Phys. Rep.* **32**, 814 (2006).
- ⁴⁸D. K. Ferry, *Semiconductor Transport* (Taylor & Francis, 2000).
- ⁴⁹V. Kolobov, R. Arslanbekov, and D. Levko, "Boltzmann-Fokker-Planck kinetic solver with adaptive mesh in phase space," e-print [arXiv:1810.09049](https://arxiv.org/abs/1810.09049).
- ⁵⁰G. A. Mesyats, "Ecton processes in the generation of pulsed runaway electron beams in a gas discharge," *Plasma Phys. Rep.* **43**, 952 (2017).
- ⁵¹V. Y. Kozhevnikov, A. V. Kozyrev, N. S. Semeniuk, and A. O. Kokovin, "Theory of a high-voltage pulse discharge in a high-pressure gas: Hydrodynamic and kinetic approaches," *Russ. Phys. J.* **61**, 603 (2018).
- ⁵²V. I. Kolobov and V. A. Godyak, "Inductively coupled plasmas at low driving frequencies," *Plasma Sources Sci. Technol.* **26**, 075013 (2017).
- ⁵³E. V. Barnat and V. I. Kolobov, "Non-monotonic radial distribution of excited atoms in a positive column of pulsed direct current discharges in helium," *Appl. Phys. Lett.* **102**, 034104 (2013).
- ⁵⁴V. Kolobov and R. Arslanbekov, "Simulation of electron kinetics in gas discharges," *IEEE Trans. Plasma Sci.* **34**, 895 (2006).
- ⁵⁵A. Tejero-del-Caz, V. Guerra, D. Gonçalves, M. L. da Silva, L. Marques, N. Pinhão, C. D. Pintassilgo, and L. L. Alves, "The Lisbon kinetics Boltzmann solver," *Plasma Sources Sci. Technol.* **28**, 043001 (2019).
- ⁵⁶I. P. Shkarofsky, T. W. Johnston, and M. P. Bachynski, *The Particle Kinetics of Plasmas* (Addison-Wesley Pub. Co., Reading, MA, 1966).
- ⁵⁷M. Capitelli, G. Colonna, G. D'Ammando, V. Laporta, and A. Laricchiuta, "The role of electron scattering with vibrationally excited nitrogen molecules on non-equilibrium plasma kinetics," *Phys. Plasmas* **20**, 101609 (2013).
- ⁵⁸C. Yuan, Z. Zhou, J. Yao, E. A. Bogdanov, A. A. Kudryavtsev, and K. M. Rabadanov, "Influence of metastable atoms on the formation of nonlocal EDF, electron reaction rates, and transport coefficients in argon plasma," *Plasma Sources Sci. Technol.* **28**, 035017 (2019).
- ⁵⁹V. I. Kolobov, "Fokker-Planck modeling of electron kinetics in plasmas and semiconductors," *Comput. Mater. Sci.* **28**, 302 (2003).
- ⁶⁰E. Bringuier, "Fokker-Planck transport simulation tool for semiconductor devices," *Philos. Mag. B* **82**, 1113 (2002).
- ⁶¹E. Bringuier, "Fokker-Planck approach to nonlocal high-field transport," *Phys. Rev. B* **54**, 5328 (1997).
- ⁶²E. Bringuier, *Electrocinetique: Transport de L'electricite Dals Les Milieu Materiels* (CNRS, 2005).
- ⁶³J. C. Dorelli and J. D. Scudder, "Electron heat flow in the solar corona: Implications of non-Maxwellian velocity distributions, the solar gravitational field, and Coulomb collisions," *J. Geophys. Res.* **108**, 1294, <https://doi.org/10.1029/2002JA009484> (2003).
- ⁶⁴C. Yuan, E. A. Bogdanov, A. A. Kudryavtsev, K. M. Rabadanov, and Z. Zhou, "Influence of electron-electron collisions on the formation of a nonlocal EDF," *Plasma Sources Sci. Technol.* **28**, 015001 (2019).
- ⁶⁵L. D. Tsendin, E. A. Bogdanov, and A. A. Kudryavtsev, "Paradoxical nonmonotonic behavior of excitation-rate spatial profiles in bounded plasmas," *Phys. Rev. Lett.* **94**, 015001 (2005).
- ⁶⁶F. Iza, G. J. Kim, S. M. Lee, J. K. Lee, J. L. Walsh, Y. T. Zhang, and M. G. Kong, "Microplasmas: Sources, particle kinetics, and biomedical applications," *Plasma Processes Polym.* **5**, 322 (2008).
- ⁶⁷I. A. Larkin, K. Keil, A. Vagov, M. D. Croitoru, and V. M. Axt, "Superanomalous skin effect for surface plasmon polaritons," *Phys. Rev. Lett.* **119**, 176801 (2017).
- ⁶⁸I. F. Voloshin, N. M. Makarov, L. M. Fisher, and V. A. Yampol'skii, "Strong nonlinear effects in conductivity of thin metallic samples," *Low Temp. Phys.* **37**, 895 (2011).
- ⁶⁹B.-W. Koo and N. Hershkowitz, "Langmuir probe in low temperature, magnetized plasmas: Theory and experimental verification," *J. Appl. Phys.* **86**, 1213 (1999).
- ⁷⁰Tsv. K. Popov, P. Ivanova, M. Dimitrova, J. Kovacic, T. Gyergyek, and M. Cercsek, "Langmuir probe measurements of the electron energy distribution function in magnetized gas discharge plasmas," *Plasma Sources Sci. Technol.* **21**, 025004 (2012).
- ⁷¹M. A. Malkov, *Plasma Diagnostics with Langmuir Probe* (SSU, Saransk, Russian Federation, 2014), p. 247 (in Russian).
- ⁷²V. I. Demidov, M. E. Koepke, I. P. Kurlyandskaya, and M. A. Malkov, "Feasibility, strategy, methodology, and analysis of probe measurements in plasma under high gas pressure," *J. Phys.: Conf. Ser.* **958**, 012003 (2018).
- ⁷³M. Usoltseva, E. Faudot, S. Devaux, S. Heurax, J. Ledig, G. V. Zaditskij, R. Ochoukov, K. Crombe, and J.-M. Noterdaeme, *Phys. Plasmas* **25**, 063518 (2018).
- ⁷⁴D. Kalita, B. Kakati, S. S. Kausik, B. K. Saikia, and M. Bandyopadhyay, "Studies on probe measurements in presence of magnetic field in dust containing hydrogen plasma," *Eur. Phys. J. D* **72**, 74 (2018).
- ⁷⁵G. Sánchez-Arriaga, "A direct Vlasov code to study the non-stationary current collection by a cylindrical Langmuir probe," *Phys. Plasmas* **20**, 013504 (2013).
- ⁷⁶G. Sánchez-Arriaga and D. Pastor-Moreno, "Direct Vlasov simulations of electron-attracting cylindrical Langmuir probes in flowing plasmas," *Phys. Plasmas* **21**, 073504 (2014).